

1 **Increased sedoheptulose-1,7-bisphosphatase content in the C₄ species *Setaria***
2 ***viridis* does not affect photosynthesis**

3

4 Maria Ermakova^{1*}, Patricia E. Lopez-Calcagno^{2,3}, Robert T. Furbank¹, Christine A. Raines², Susanne
5 von Caemmerer¹.

6

7 ¹Centre of Excellence for Translational Photosynthesis, Division of Plant Science, Research School of
8 Biology, The Australian National University, Canberra Australian Capital Territory, 2600, Australia.

9 ² School of Biological Sciences, University of Essex, Wivenhoe Park, Colchester, CO4 3SQ, UK.

10 ³ School of Natural and Environmental Sciences, Newcastle University, Newcastle, NE1 7RU, UK.

11

12 *Corresponding author: Maria Ermakova, maria.ermakova@anu.edu.au.

13

14 Running head: Role of SBPase in C₄ photosynthesis

15 **Abstract**

16 Sedoheptulose-1,7-bisphosphatase (SBPase) is one of the rate-limiting enzymes of the Calvin cycle,
17 and, in C₃ plants, increasing the abundance of SBPase is known to provide higher photosynthetic
18 rates and stimulate biomass and yield. C₄ plants usually have higher photosynthetic rates because
19 they operate a biochemical CO₂ concentrating mechanism between mesophyll and bundle sheath
20 cells. In the C₄ system, SBPase and other enzymes of Calvin cycle are localised to the bundle sheath
21 cells. Here we tested what effect increasing abundance of SBPase would have on C₄ photosynthesis.
22 Using *Setaria viridis*, a model C₄ plant of NADP-ME subtype, we created transgenic plants with 1.5
23 to 3.2-times higher SBPase content, compared to wild type plants. Transcripts of the transgene were
24 found predominantly in the bundle sheaths suggesting the correct cellular localisation of the
25 protein. Abundance of RBCL, the large subunit of Rubisco, was not affected in transgenic plants
26 overexpressing SBPase, and neither was relative chlorophyll content or photosynthetic electron
27 transport parameters. We found no correlation between SBPase content in *S. viridis* and saturating
28 rates of CO₂ assimilation. Moreover, detailed analysis of CO₂ assimilation rates at different CO₂
29 partial pressure, irradiance and leaf temperature, showed no improvement of photosynthesis in
30 plants overexpressing SBPase. We discuss potential implications of these results for understanding
31 the regulation of C₄ photosynthesis.

32

33 **Keywords:** C₄ photosynthesis, SBPase, CO₂ assimilation, Calvin cycle, bundle sheath cells.

34

35 **Introduction**

36 Global crop production needs to double by 2050 to meet the projected demands from a rising
37 population, diet shifts, and increasing biofuels consumption (Ray et al., 2013). Increasing
38 photosynthetic capacity of plants was proposed to significantly increase crop yield (Long et al., 2006,
39 Parry et al., 2013, Evans, 2013, Bailey-Serres et al., 2019, Ort et al., 2015, Raines, 2011, Simkin et al.,
40 2019). This has led to research efforts focusing on improving various photosynthetic components in
41 attempt to improve plant productivity (Kromdijk et al., 2016, Ermakova et al., 2021b, López-
42 Calcagno et al., 2019, Lefebvre et al., 2005, South et al., 2019, López-Calcagno et al., 2020).

43 The Calvin-Benson-Bassham (C₃) cycle is the primary pathway for CO₂ fixation in all terrestrial plants.
44 This cycle plays a central role in plant metabolism providing intermediates for starch and sucrose
45 synthesis as well as isoprenoid metabolism and the shikimic acid biosynthesis (Geiger and Servaites,
46 1994). Manipulation of C₃-cycle enzymes has led to increases in photosynthetic rates (reviewed by

47 Simkin et al., 2019). In particular, overexpression of sedoheptulose-1,7-bisphosphatase (SBPase) in
48 several C₃ species has led to increases in photosynthetic rates and increased biomass in the
49 laboratory and the field (Rosenthal et al., 2011, Lefebvre et al., 2005, Driever et al., 2017, Feng et
50 al., 2007, Ding et al., 2016). SBPase catalyses the dephosphorylation of sedoheptulose-1,7-
51 bisphosphate, the reaction nested at the branch point between the regenerative phase of the C₃
52 cycle and sucrose or starch biosynthesis. Due to this unique position, SBPase is one of the critical
53 enzymes controlling the carbon flow in plants (Raines et al., 2000).

54 A major limitation of the C₃ cycle is the enzyme ribulose-1,5-bisphosphate carboxylase/oxygenase
55 (Rubisco) catalysing the fixation of CO₂ into ribulose-1,5-bisphosphate (RuBP) producing glyceral-
56 3-phosphate, a 3-C compound giving the name 'C₃ species' to those that use this cycle exclusively.
57 However, Rubisco also catalyses an oxygenase reaction that competes with CO₂ fixation resulting in
58 reductions in yield of over 25% (Walker et al., 2016). To get around this problem, ~ 4 % of plant
59 species have evolved a biochemical CO₂ concentrating mechanism, called the C₄ pathway, that
60 operates in addition to the C₃ cycle and involves two functionally distinct cell types. In the C₄
61 pathway, atmospheric CO₂ diffuses into the leaf mesophyll cells where it is converted to HCO₃⁻ by
62 carbonic anhydrase (CA) which is then fixed by phosphoenolpyruvate (PEP) carboxylase (PEPC) to
63 produce C₄ acids (giving the name to this pathway). These C₄ acids diffuse into the bundle sheath
64 cells where they are decarboxylated, thereby elevating the CO₂ partial pressure (pCO₂) where
65 Rubisco is located, allowing Rubisco to operate close to its maximal rate (Hatch, 1987). C₄ crops are
66 high yielding and are characterised by high photosynthetic rates, high nitrogen and water use
67 efficiency when compared to plants using only the C₃ cycle. This has stimulated considerable interest
68 in the C₄ photosynthetic pathway (Mitchell and Sheehy, 2006), and a range of strategies to
69 manipulate and enhance C₄ photosynthesis are also being considered (von Caemmerer and Furbank,
70 2016). The rate of Rubisco catalysis and the regeneration of PEP and RuBP together with the electron
71 transport capacity are all possible limiting factors of C₄ photosynthesis under high pCO₂ and high
72 irradiance conditions (von Caemmerer and Furbank, 2016).

73 To explore these limitations, a new model species, *Setaria viridis* (green foxtail millet), has emerged
74 to enable the study of C₄ plant biology. Like the major C₄ crops maize (*Zea mays*) and sorghum, *S.*
75 *viridis* belongs to the NADP-ME decarboxylation C₄ subtype and is readily transformable opening
76 opportunities to investigate the possibility of enhancing C₄ photosynthesis (Brutnell et al., 2010).
77 Overexpression of the Rieske FeS protein in *S. viridis* has been shown to enhance C₄ photosynthesis
78 (Ermakova et al., 2019) and the joint overexpression of Rubisco subunits with the RUBISCO
79 ASSEMBLY FACTOR 1 in *Z. mays* has increased Rubisco protein content and photosynthetic rate

80 (Salesse-Smith et al., 2018). Given that the C₃ cycle plays an equally important role in C₄ plants and
81 the success reported in enhancing C₃ photosynthesis by increasing SBPase content, here we
82 investigated whether overexpression of SBPase could also enhance C₄ photosynthesis. To test this
83 hypothesis, we produced and analysed *S. viridis* plants expressing *Brachypodium distachyon* SBPase
84 using a bundle sheath cell-preferential promoter. Our results showed that SBPase content does not
85 limit C₄ photosynthetic flux under any of the environmental conditions tested.

86 **Materials and Methods**

87 **Generating transgenic plants**

88 The coding sequence of *Brachypodium distachyon* SBPase (Bradi2g55150, [https://phytozome-](https://phytozome-next.jgi.doe.gov)
89 [next.jgi.doe.gov](https://phytozome-next.jgi.doe.gov)) was codon-optimised for the Golden Gate cloning system (Engler et al., 2014) and
90 assembled with the bundle sheath cell-preferential *Flaveria trinervia* GLDP (glycine decarboxylase
91 P-protein) promoter (Engelmann et al., 2008, Gupta et al., 2020) and the bacterial *NOS* (nopaline
92 synthase) terminator. The resulting expression module was cloned into the second slot of a plant
93 binary vector pAGM4723. The first slot was occupied by the *hpt* (hygromycin phosphotransferase)
94 gene driven by the *Oryza sativa* *Actin1* promoter. The construct was verified by sequencing and
95 transformed into *Setaria viridis* cv. MEO V34-1 using *Agrobacterium tumefaciens* strain AGL1
96 according to the protocol described in detail in Osborn et al. (2016). T₀ plants resistant to
97 hygromycin were transferred to soil and tested for SBPase abundance by immunoblotting and *hpt*
98 copy number by droplet digital PCR (iDNA genetics, Norwich, UK). Wild type (WT) plants were used
99 as control in all experiments.

100 **Plant growth conditions**

101 Seeds were surface-sterilized and germinated on rooting medium containing 2.15 g L⁻¹ Murashige
102 and Skoog salts, 10 ml L⁻¹ 100x Murashige and Skoog vitamins stock, 30 g L⁻¹ sucrose, 7 g L⁻¹
103 Phytoblend, 20 mg L⁻¹ hygromycin (no hygromycin for WT plants), pH 5.7. Seedlings that developed
104 secondary roots were transferred to 1 L pots with the commercial potting mix (Debco, Tyabb,
105 Australia) layered on top with 2 cm of the seed raising mix (Debco) both containing 1 g L⁻¹ Osmocote
106 (Scotts, Bella Vista, Australia). Plants were grown in controlled environment chambers with ambient
107 CO₂, 16 h photoperiod, 28 °C day, 22 °C night and 60 % humidity. Light at the intensity of 300 μmol
108 m⁻² s⁻¹ was supplied by 1000 W red sunrise 3200K lamps (Sunmaster Growlamps, Solon, OH).
109 Youngest fully expanded leaves of 3 weeks-old plants were used in all experiments. Photosynthetic
110 and physiological parameters of leaves were measured with the MultispeQ using 'Photosynthesis

111 RIDES' protocol at ambient conditions in the growth chamber (Kuhlgert et al., 2016). The results
112 were analysed using the PhotosynQ platform (<https://photosynq.com>).

113 **Immunoblotting**

114 Leaf discs of the same area were collected and immediately frozen in liquid N₂. Protein samples
115 were isolated from leaf discs as described in Ermakova et al. (2019). Proteins were separated by
116 SDS-PAGE, transferred to a nitrocellulose membrane and probed with antibodies against SBPase
117 (AS152873, Agrisera, Vännäs, Sweden), RBCL (Martin-Avila et al., 2020) and PEPC (Karki et al., 2020).
118 Quantification of immunoblots was performed with the Image Lab software (Biorad, Hercules, CA).

119 **Bundle sheath isolation and qPCR**

120 BS strands were isolated following the procedure of Ghannoum et al. (2005) as described in detail
121 in Ermakova et al. (2021a). RNA was isolated from leaves and BS strands, ground in liquid N₂, using
122 the RNeasy Plant Mini Kit (Qiagen, Venlo, The Netherlands). DNA was removed from the samples
123 using the Ambion TURBO DNA free kit (Thermo Fisher Scientific, Tewksbury, MA). cDNA was
124 synthesised and analysed by qPCR as described in (add ref Ermakova 2019). Relative fold change
125 was calculated by the $\Delta\Delta C_t$ method using the geometric mean of the C_t values for three reference
126 genes described in Osborn et al. (2016). Primers to distinguish between *S. viridis* and *B. distachyon*
127 SBPase transcripts were designed using Primer3 in Geneious R9.1.1 (<https://www.geneious.com>).

128 **Gas Exchange**

129 Gas exchange analysis was performed using a LI-6800 (LI-COR Biosciences, Lincoln, NE). First, leaves
130 were equilibrated at 1500 $\mu\text{mol m}^{-2} \text{s}^{-1}$ (90 % red / 10 % blue actinic light), 400 ppm CO₂ in the
131 reference side, leaf temperature 28 °C, 60% humidity and flow rate of 500 $\mu\text{mol s}^{-1}$, and then light
132 or CO₂ response curves of CO₂ assimilation were recorded. For the light response curves, a stepwise
133 increase of irradiance from 0 to 3000 $\mu\text{mol m}^{-2} \text{s}^{-1}$ was imposed at 2-min intervals. For the CO₂
134 response curves, a stepwise increase of CO₂ partial pressures from 0 to 1600 ppm was imposed at
135 3-min intervals. To record CO₂ response curves at different temperatures, plants were kept in
136 growth cabinets set to 15 °C or 35 °C, and leaves were equilibrated at a corresponding leaf
137 temperature for 20 min before the measurement.

138 **Statistical analysis**

139 The relationship between mean values of transgenic and WT plants was tested using two-tailed,
140 heteroscedastic Student's *t*-test.

141 **Results**

142 Six *S. viridis* plants resistant to hygromycin were regenerated after the transformation with the
143 construct for SBPase overexpression. The *hpt* copy number identified by the digital PCR indicated

144 that T_0 plants contained one to three *B. distachyon* SBPase (*BdSBPase*) copies (Fig. 1a).
145 Immunodetection of SBPase and PEPC suggested increased SBPase abundance, relative to PEPC, in
146 multiple T_0 plants when compared to WT. Plants 2, 3 and 5 were selected and the progeny of these
147 lines was further analysed. To verify bundle sheath cell-preferential expression of *BdSBPase*, total
148 RNA was isolated from leaves and bundle sheath strands of WT plants and homozygous T_1 plants of
149 line 3. Transcript abundance of *BdSBPase* and the native SBPase (*SvSBPase*) in the bundle sheaths
150 exceeded the levels detected from whole leaves indicating that both genes were preferentially
151 expressed in bundle sheath cells (Fig. 1b).

152 We studied the impact of increased SBPase abundance on C_4 photosynthesis first by analysing T_1
153 plants of lines 2 and 3 for *hpt* insertion number and SBPase and Rubisco large subunit (RBCL)
154 content. Relative abundance of SBPase, quantified from the immunoblots (Fig. 2a), showed strong
155 positive correlation with the insertion number in T_1 plants and, thus, with the copy number of
156 *BdSBPase* (Fig. 2b). Homozygous plants of line 2, containing four copies of *BdSBPase*, showed the
157 highest SBPase levels (about four times of WT). Relative content of RBCL showed no correlation with
158 the insertion number (Fig. 2c) indicating that neither increased SBPase abundance or insertion
159 positions had an impact on Rubisco abundance in transgenic plants. In addition, neither relative Chl
160 abundance or leaf thickness was affected in plants with increased SBPase content, compared to WT
161 (Table 1).

162 Next, we studied photosynthetic properties of *S. viridis* plants with increased SBPase content. Figure
163 3 shows that CO_2 assimilation rates measured from WT and T_1 plants of lines 2 and 3 at ambient CO_2
164 partial pressure were not affected by SBPase content, quantified from the immunoblots (Fig. 2a).
165 Moreover, no difference in CO_2 assimilation rates was detected between WT and transgenic plants
166 overexpressing SBPase at different intercellular CO_2 partial pressures or irradiances (Fig. 4). Electron
167 transport parameters measured at growth light intensity indicated that plants with increased
168 SBPase content had WT-like activity of Photosystem II, since no changes in partitioning of the
169 absorbed light between photochemical (PhiPSII) and non-photochemical (PhiNPQ and PhiNO)
170 reactions within Photosystem II were detected (Table 1). Activity of the chloroplast ATP synthase,
171 estimated as the proton conductivity of thylakoid membrane (g_{H^+}), did not differ between the
172 genotypes either (Table 1).

173 We also tested CO_2 assimilation rates at different temperature in homozygous T_2 plants of lines 3
174 and 5 with increased SBPase abundance confirmed by immunoblotting (Fig. S1). For this, CO_2
175 response curves of assimilation were measured on leaves acclimated to 35 °C and at 15 °C (Fig. 5).
176 No difference in CO_2 assimilation was detected between WT and transgenic plants overexpressing

177 SBPase at 35 °C. At 15 °C, both transgenic lines showed WT-like rates of assimilation, except for the
178 plants of line 5 having significantly increased CO₂ assimilation rate of 6.80 ± 0.04 μmol m⁻² s⁻¹ at the
179 intercellular CO₂ partial pressure of about 13 μbar, compared to the WT rate of 5.14 ± 0.35 μmol m⁻²
180 s⁻¹ ($P = 0.040$, *t*-test).

181 Discussion

182 Overexpression of SBPase has led to increases in photosynthetic rates and increased biomass in
183 several C₃ species (Rosenthal et al., 2011, Lefebvre et al., 2005, Driever et al., 2017, Feng et al., 2007,
184 Ding et al., 2016). In the C₄ photosynthetic system, SBPase and the C₃ cycle are located in the bundle
185 sheath cells, and therefore the C₃ cycle in C₄ photosynthesis is poised differently to the C₃ cycle in
186 C₃ species. Because the C₃ cycle operates at high CO₂ partial pressure in the bundle sheath, C₄
187 species have characteristically less Rubisco protein than C₃ species (Sage and Pearcy, 1987, von
188 Caemmerer and Furbank, 2016), however to achieve high photosynthetic rates SBPase levels will
189 need to be similar to that in C₃ species.

190 Here we expressed *BdSBPase* from a bundle sheath cell-preferential promoter to test SBPase
191 overexpression in a C₄ photosynthetic system. We observed increased SBPase content in T₀ plants
192 and selected 3 T₁ lines for our investigations (Fig. 1). Transgenic plants had between 1.5 to 3.2 times
193 the amount of SBPase, relative to WT, as judged from the immunoblots (Fig. 2a, Fig. S1). Despite
194 these significant increases in protein content, we observed no increase in photosynthetic rates
195 under a range of environmental conditions including different irradiances, *p*CO₂ and temperatures.
196 The C₄ photosynthetic model suggests that SBPase limitation should be apparent at *p*CO₂ above
197 ambient where SBPase content may well be co-limiting with electron transport capacity, Rubisco
198 activity and PEP regeneration (von Caemmerer, 2021, von Caemmerer and Furbank, 1999).

199 *S. viridis* uses NADPH-dependent malic enzyme (NADP-ME) decarboxylation system in the bundle
200 sheath chloroplast (Fig. 6) and, similar to most of NADP-ME species, *S. viridis* has low PSII activity
201 and linear electron transport rate in bundle sheath cells (Ermakova et al., 2021a). This prompts
202 export of part of the 3-phosphoglycerate (3-PGA) pool to the mesophyll for conversion to triose
203 phosphate, which then diffuses back to the bundle sheath, known as the triose phosphate shuttle
204 (von Caemmerer and Furbank, 2016 and references therein) (Fig. 6). To support this movement of
205 triose phosphate and 3-PGA, diffusion gradients between the mesophyll cells and the bundle sheath
206 must be built up and maintained (Furbank and Kelly, 2021 and references therein). Moreover,
207 reactions of sucrose and starch synthesis are distributed between the different cell types in the C₄
208 system with sucrose being made mostly in the mesophyll cells and starch - in the bundle sheaths

209 (Furbank et al., 1985, Lunn and Furbank, 1997, Furbank and Kelly, 2021). The combination of the
210 triose phosphate shuttle and the cellular localisation of sucrose and starch biosynthesis may mean
211 that regulation of the regeneration of RuBP in C₄ bundle sheath chloroplasts is somewhat different
212 to that in C₃ chloroplasts where sucrose and starch synthesis and 3-PGA reduction are all occurring
213 in a single cell type. It has been proposed that both SBPase and FBPase play key roles in determining
214 the fate of triose phosphate in the C₃ cycle, *i.e.*, whether it is recycled to regenerate RuBP or used
215 to make sucrose and starch (Raines et al., 2000 and references therein). This regulation is important
216 as the metabolite pools within the cycle need to be preserved and flux maintained while carbon is
217 removed for storage. Because of the, this regulation is controlled not only by the activities of these
218 biphosphatases but by a complex balance of orthophosphate consumption in photophosphorylation
219 and its resupply from P_i release in sucrose biosynthesis and the activity of ADPG-pyrophosphorylase
220 (Furbank and Kelly, 2021). Since in the C₄ bundle sheath chloroplast, triose phosphate is imported
221 in exchange for 3-PGA export, the P_i recycling process is by necessity different to the C₃ case where
222 triose phosphate is exchanged for P_i. This division of metabolism between the cell types and the
223 higher flexibility of carbon flow in C₄ plants might reduce the capacity to regulate carbon flux by the
224 abundance of SBPase.

225 Little is known about potential differences in regulation of SBPase between C₃ and C₄ plants. There
226 is evidence that the kinetic properties of enzymes such as cytosolic FBPase are quite different in C₄
227 plants to support the cellular gradients required for fluxes of metabolites (Furbank and Kelly, 2021).
228 Wheat SBPase was shown to be regulated by pH and Mg²⁺ concentrations consistent with its activity
229 being stimulated under light (Woodrow et al., 1984). Moreover, like some other enzymes of the C₃
230 cycle, SBPase is activated by the thioredoxin system via a light-dependent reduction of the disulfide
231 bond (Breazeale et al., 1978, Dunford et al., 1998). Since we were not able to measure *in vitro*
232 activity of SBPase, there is a possibility that SBPase from *B. distachyon*, a C₃ plant, was inactive when
233 expressed in the bundle sheath cells of C₄ plant. However, the amino acid sequences of SBPase from
234 *S. viridis* and *B. distachyon* are 92.4 % identical, and all cysteine residues are conserved (Fig. S2).
235 Moreover, SBPase from *Z. mays* could be activated by thioredoxin *f* from spinach suggesting a cross-
236 reactivity between enzymes and thioredoxins from different species (Nishizawa and Buchanan,
237 1981). Nevertheless, although a positive correlation was typically observed between the active form
238 and total enzyme abundance in C₃ plants overexpressing SBPase (Driever et al., 2017), there is a
239 possibility that the 'extra' SBPase is not activated in *S. viridis* due to a limited availability of reducing
240 power to the thioredoxin system in C₄ bundle sheath cells. In that case, C₄ photosynthesis would not

241 be limited by SBPase directly, but rather by electron transport, which has been previously confirmed
242 (Ermakova et al., 2019).

243 **Conclusion**

244 Under the range of conditions tested in this study, increasing SBPase levels did not increase
245 photosynthetic flux in the C₄ grass *Setaria viridis*, in contrast to observations of SBPase
246 overexpression in C₃ plants. We propose that this is because of (i) the triose phosphate shuttle in C₄
247 plants, where part of the 3-PGA produced by Rubisco is reduced in the mesophyll chloroplasts and
248 returned to the bundle sheath chloroplasts, and (ii) the cellular specialisation of starch and sucrose
249 biosynthesis in C₄ leaves where these processes are spatially separated. These unique aspects of the
250 C₄ photosynthetic pathway are likely to result in a different distribution of control over regeneration
251 of RuBP and the coordination of RuBP production and sugar phosphate utilisation in starch and
252 sucrose synthesis. At present, the degree of sophistication of the C₄ photosynthetic model is
253 insufficient to accommodate these finely tuned control mechanisms.

254

255 **Table 1.** Photosynthetic and physiological parameters measured on leaves of wild type (WT) *S. viridis*
256 and two transgenic lines overexpressing SBPase at growth light intensity. PhiPSII, the effective
257 quantum yield of Photosystem II; PhiNPQ, the yield of non-photochemical quenching; PhiNO, the
258 yield of non-regulated non-photochemical reactions in PSII; g_{H^+} , proton conductivity of the thylakoid
259 membrane. Mean \pm SE, n = 6-7 biological replicates. No statistically significant differences were
260 found between transgenic and WT plants ($P < 0.05$).

261

Parameter	WT	Line 2	Line 3
Relative Chl (SPAD)	43.57 \pm 0.83	42.02 \pm 1.18	43.00 \pm 0.95
Leaf thickness, mm	0.59 \pm 0.08	0.64 \pm 0.07	0.58 \pm 0.09
PhiPSII	0.62 \pm 0.01	0.62 \pm 0.01	0.63 \pm 0.02
PhiNO	0.21 \pm 0.01	0.20 \pm 0.01	0.20 \pm 0.01
PhiNPQ	0.17 \pm 0.01	0.18 \pm 0.01	0.17 \pm 0.01
g_{H^+}	240.4 \pm 18.2	239.4 \pm 7.2	255.1 \pm 15.2

262

263

264 Figure legends

265 **Figure 1.** Selection of *S. viridis* plants overexpressing SBPase. **a.** Immunoblots of SBPase and PEPC in
266 WT *S. viridis* and 6 T₀ plants transformed with *SBPase* from *Brachypodium distachyon* under the
267 control of the bundle sheath cell-preferential *GLDP* promoter. The *hpt* copy numbers estimated by
268 digital PCR and suggesting the *BdSBPase* insertion numbers are also shown. Asterisks indicate the
269 plants which progenies were used in further experiments. **b.** Transcript abundance of *S. viridis*
270 *SBPase* (*SvSBPase*) and *B. distachyon* *SBPase* (*BdSBPase*) in whole leaf tissue and isolated bundle
271 sheath strands (BS) shows bundle sheath-preferential localisation of the native gene and transgene
272 transcripts. Mean ± SE, *n* = 3 biological replicates.

273 **Figure 2.** Analysis of *S. viridis* plants overexpressing SBPase. **a.** Immunodetection of SBPase and RBCL
274 in protein samples isolated from leaves of WT plants and the T₁ progeny of transgenic lines 2 and 3.
275 Samples were loaded on leaf area basis, and the titration series of the WT1 sample was used for
276 relative quantification. Insertion number indicates *hpt* copy number estimated by digital PCR. **b** and
277 **c.** Relative SBPase and RBCL content as a function of insertion number (data taken from a).

278 **Figure 3.** Saturating CO₂ assimilation rate as a function of relative SBPase content in leaves of WT *S.*
279 *viridis* and T₁ progeny of lines 2 and 3 overexpressing SBPase. Measurements were made at an
280 ambient CO₂ partial pressure of 400 µbar, an irradiance of 1500 µmol m⁻² s⁻¹ and a leaf temperature
281 of 28 °C.

282 **Figure 4.** Gas exchange properties of WT *S. viridis* and transgenic plants overexpressing SBPase. **a.**
283 CO₂ assimilation rate as a function of intercellular CO₂ partial pressure. Measurements were made
284 at an irradiance of 1500 µmol m⁻² s⁻¹ and a leaf temperature of 28 °C. **b.** CO₂ assimilation rate as a
285 function of irradiance. Measurements were made at an ambient CO₂ partial pressure of 400 µbar
286 and a leaf temperature of 28 °C. Measurements were made on the T₁ progeny of lines 2 and 3.
287 Average relative abundance of SBPase per leaf area, calculated from immunoblots on Fig. 2, was
288 significantly increased in line 2 (3.2 times, *P* = 0.002) and in line 3 (2.0 times, *P* = 0.001), relative to
289 WT. Mean ± SE, *n* = 3 biological replicates. No significant differences were found (*P* < 0.05).

290 **Figure 5.** CO₂ assimilation rate as a function of intercellular CO₂ partial pressure at different
291 temperatures in WT *S. viridis* and transgenic plants overexpressing SBPase. Measurements were
292 made at an irradiance of 1500 µmol m⁻² s⁻¹ and a leaf temperature of 35 °C or 15 °C. Measurements
293 were made on the T₂ progeny of lines 3 and 5 and wild type. Average relative abundance of SBPase
294 per leaf area, calculated from immunoblots on Fig. S1, was increased 2 times in line 3 and 1.5 times

295 in line 5, relative to WT. Mean \pm SE, $n = 3$ biological replicates. Details of statistical analysis are
296 provided in the results.

297 **Figure 6.** Schematic of the NADP-ME C₄ photosynthetic pathway of *S. viridis* showing the location of
298 SBPase in the pathway.

299 **Acknowledgements**

300 We thank Xueqin Wang for help with *S. viridis* transformation, Zac Taylor and Ayla Manwaring for
301 immunoblotting and Emily Watson for gas exchange measurements. This work was supported by
302 the Australian Research Council Centre of Excellence in Translational Photosynthesis
303 (CE140100015).

304 **Author Contributions**

305 SvC, CR, RF and ME designed the research; ME and PL performed research; ME and SvC analysed
306 data; SvC, ME, CR and RF wrote the paper.

307 **Conflict of Interest**

308 Authors declare no conflict of interest.

309 **References**

311 BAILEY-SERRES, J., PARKER, J. E., AINSWORTH, E. A., OLDROYD, G. E. D. & SCHROEDER, J. I. 2019.
312 Genetic strategies for improving crop yields. *Nature*, 575, 109-118.

313 BREAZEALE, V. D., BUCHANAN, B. B. & WOLOSIUK, R. A. 1978. Chloroplast Sedoheptulose 1,7-
314 Bisphosphatase: Evidence for Regulation by the Ferredoxin/Thioredoxin System. *Zeitschrift
für Naturforschung C*, 33, 521-528.

315 BRUTNELL, T. P., WANG, L., SWARTWOOD, K., GOLDSCHMIDT, A., JACKSON, D., ZHU, X. G.,
316 KELLOGG, E. & VAN ECK, J. 2010. Setaria viridis: A Model for C₄ Photosynthesis. *Plant Cell*,
317 22, 2537-2544.

318 DING, F., WANG, M., ZHANG, S. & AI, X. 2016. Changes in SBPase activity influence photosynthetic
319 capacity, growth, and tolerance to chilling stress in transgenic tomato plants. *Scientific
Reports*, 6, 32741.

320 DRIEVER, S. M., SIMKIN, A. J., ALOTAIBI, S., FISK, S. J., MADGWICK, P. J., SPARKS, C. A., JONES, H.
321 D., LAWSON, T., PARRY, M. A. J. & RAINES, C. A. 2017. Increased SBPase activity improves
322 photosynthesis and grain yield in wheat grown in greenhouse conditions. *Philosophical
Transactions of the Royal Society B: Biological Sciences*, 372, 20160384.

323 DUNFORD, R. P., CATLEY, M. A., RAINES, C. A., LLOYD, J. C. & DYER, T. A. 1998. Purification of
324 Active Chloroplast Sedoheptulose-1,7-Bisphosphatase Expressed in *Escherichia coli*. *Protein
Expression and Purification*, 14, 139-145.

325 ENGELMANN, S., WILUDDA, C., BURSCHEIDT, J., GOWIK, U., SCHLUE, U., KOCZOR, M., STREUBEL,
326 M., COSSU, R., BAUWE, H. & WESTHOFF, P. 2008. The gene for the P-subunit of glycine

331 decarboxylase from the C₄ species *Flaveria trinervia*: Analysis of transcriptional control in
332 transgenic *Flaveria bidentis* (C₄) and *Arabidopsis* (C₃). *Plant Physiology*, 146, 1773-1785.

333 ENGLER, C., YOULES, M., GRUETZNER, R., EHNERT, T.-M., WERNER, S., JONES, J. D. G., PATRON, N.
334 J. & MARILLONNET, S. 2014. A Golden Gate Modular Cloning Toolbox for Plants. *ACS
335 Synthetic Biology*, 3, 839-843.

336 ERMAKOVA, M., BELLASIO, C., FITZPATRICK, D., FURBANK, R., MAMEDOV, F. & VON CAEMMERER,
337 S. 2021a. Upregulation of bundle sheath electron transport capacity under limiting light in
338 C₄ *Setaria viridis*. *The Plant Journal*, 106, 1443-1454.

339 ERMAKOVA, M., LOPEZ-CALCAGNO, P. E., RAINES, C. A., FURBANK, R. T. & VON CAEMMERER, S.
340 2019. Overexpression of the Rieske FeS protein of the Cytochrome b₆f complex increases
341 C₄ photosynthesis in *Setaria viridis*. *Communications Biology* 2.

342 ERMAKOVA, M., OSBORN, H., GROSZMANN, M., BALA, S., BOWERMAN, A., MCGAUGHEY, S., BYRT,
343 C., ALONSO-CANTABRANA, H., TYERMAN, S., FURBANK, R. T., SHARWOOD, R. E. & VON
344 CAEMMERER, S. 2021b. Expression of a CO₂-permeable aquaporin enhances mesophyll
345 conductance in the C₄ species *Setaria viridis*. *eLife*, 10, e70095.

346 EVANS, J. R. 2013. Improving Photosynthesis. *Plant Physiology*, 162, 1780-1793.

347 FENG, L. L., WANG, K., LI, Y., TAN, Y. P., KONG, J., LI, H., LI, Y. S. & ZHU, Y. G. 2007. Overexpression
348 of SBPase enhances photosynthesis against high temperature stress in transgenic rice
349 plants. *Plant Cell Reports*, 26, 1635-1646.

350 FURBANK, R. T. & KELLY, S. 2021. Finding the C₄ sweet spot: cellular compartmentation of
351 carbohydrate metabolism in C₄ photosynthesis. *Journal of Experimental Botany*, 72, 6018-
352 6026.

353 FURBANK, R. T., STITT, M. & FOYER, C. H. 1985. Intercellular compartmentation of sucrose
354 synthesis in leaves of *Zea mays* L. *Planta*, 164, 172-178.

355 GEIGER, D. R. & SERVAITES, J. C. 1994. Diurnal regulation of photosynthetic carbon metabolism in
356 C₃ plants. *Annual Review of Plant Physiology and Plant Molecular Biology*, 45, 235-256.

357 GHANNOUM, O., EVANS, J. R., CHOW, W. S., ANDREWS, T. J., CONROY, J. P. & VON CAEMMERER,
358 S. 2005. Faster Rubisco Is the Key to Superior Nitrogen-Use Efficiency in NADP-Malic
359 Enzyme Relative to NAD-Malic Enzyme C₄ Grasses. *Plant Physiology*, 137, 638-
360 650.

361 GUPTA, S. D., LEVEY, M., SCHULZE, S., KARKI, S., EMMERLING, J., STREUBEL, M., GOWIK, U., PAUL
362 QUICK, W. & WESTHOFF, P. 2020. The C₄Ppc promoters of many C₄ grass species share a
363 common regulatory mechanism for gene expression in the mesophyll cell. *The Plant
364 Journal*, 101, 204-216.

365 HATCH, M. D. 1987. C₄ photosynthesis: A unique blend of modified biochemistry, anatomy and
366 ultrastructure. *Biochim.Biophys.Acta*, 895, 81-106.

367 KARKI, S., LIN, H., DANILA, F. R., ABUJAMOUS, B., GIULIANI, R., EMMS, D. M., COE, R. A.,
368 COVSHOFF, S., WOODFIELD, H., BAGUNU, E., THAKUR, V., WANCHANA, S., SLAMET-
369 LOEDIN, I., COUSINS, A. B., HIBBERD, J. M., KELLY, S. & QUICK, W. P. 2020. A role for neutral
370 variation in the evolution of C₄ photosynthesis. *bioRxiv*, 2020.05.19.104299.

371 KROMDIJK, J., GŁOWACKA, K., LEONELLI, L., GABILLY, S. T., IWAI, M., NIYOGI, K. K. & LONG, S. P.
372 2016. Improving photosynthesis and crop productivity by accelerating recovery from
373 photoprotection. *Science*, 354, 857-861.

374 KUHLGERT, S., AUSTIC, G., ZEGARAC, R., OSEI-BONSU, I., HOH, D., CHILVERS MARTIN, I., ROTH
375 MITCHELL, G., BI, K., TERAVEST, D., WEEBADDE, P. & KRAMER DAVID, M. 2016. MultispeQ
376 Beta: a tool for large-scale plant phenotyping connected to the open PhotosynQ network.
377 *Royal Society Open Science*, 3, 160592.

378 LEFEBVRE, S., LAWSON, T., ZAKHLENIUK, O. V., LLOYD, J. C. & RAINES, C. A. 2005. Increased
379 sedoheptulose-1,7-bisphosphatase activity in transgenic tobacco plants stimulates

380 photosynthesis and growth from an early stage in development. *Plant Physiology*, 138,
381 451-460.

382 LONG, S. P., ZHU, X. G., NAIDU, S. L. & ORT, D. R. 2006. Can improvement in photosynthesis
383 increase crop yields? *Plant Cell and Environment*, 29, 315-330.

384 LÓPEZ-CALCAGNO, P. E., BROWN, K. L., SIMKIN, A. J., FISK, S. J., VIALET-CHABRAND, S., LAWSON, T.
385 & RAINES, C. A. 2020. Stimulating photosynthetic processes increases productivity and
386 water-use efficiency in the field. *Nature Plants*, 6, 1054-1063.

387 LÓPEZ-CALCAGNO, P. E., FISK, S., BROWN, K. L., BULL, S. E., SOUTH, P. F. & RAINES, C. A. 2019.
388 Overexpressing the H-protein of the glycine cleavage system increases biomass yield in
389 glasshouse and field-grown transgenic tobacco plants. *Plant Biotechnology Journal*, 17,
390 141-151.

391 LUNN, J. E. & FURBANK, R. T. 1997. Localisation of sucrose-phosphate synthase and starch in
392 leaves of C-4 plants. *Planta*, 202, 106-111.

393 MARTIN-AVILA, E., LIM, Y.-L., BIRCH, R., DIRK, L. M. A., BUCK, S., RHODES, T., SHARWOOD, R. E.,
394 KAPRALOV, M. V. & WHITNEY, S. M. 2020. Modifying Plant Photosynthesis and Growth via
395 Simultaneous Chloroplast Transformation of Rubisco Large and Small Subunits. *The Plant
396 Cell*, 32, 2898-2916.

397 MITCHELL, P. L. & SHEEHY, J. E. 2006. Supercharging rice photosynthesis to increase yield. *New
398 Phytologist*, 171, 688-693.

399 NISHIZAWA, A. N. & BUCHANAN, B. B. 1981. Enzyme regulation in C4 photosynthesis. Purification
400 and properties of thioredoxin-linked fructose bisphosphatase and sedoheptulose
401 bisphosphatase from corn leaves. *Journal of Biological Chemistry*, 256, 6119-6126.

402 ORT, D. R., MERCHANT, S. S., ALRIC, J., BARKAN, A., BLANKENSHIP, R. E., BOCK, R., CROCE, R.,
403 HANSON, M. R., HIBBERD, J. M., LONG, S. P., MOORE, T. A., MORONEY, J., NIYOGI, K. K.,
404 PARRY, M. A. J., PERALTA-YAHYA, P. P., PRINCE, R. C., REDDING, K. E., SPALDING, M. H.,
405 VAN WIJK, K. J., VERMAAS, W. F. J., VON CAEMMERER, S., WEBER, A. P. M., YEATES, T. O.,
406 YUAN, J. S. & ZHU, X. G. 2015. Redesigning photosynthesis to sustainably meet global food
407 and bioenergy demand. *Proceedings of the National Academy of Sciences of the United
408 States of America*, 112, 8529-8536.

409 OSBORN, H. L., EVANS, J. R., SHARWOOD, R. E., FURBANK, R. T., VON CAEMMERER, S., ALONSO-
410 CANTABRANA, H. & COVSHOFF, S. 2016. Effects of reduced carbonic anhydrase activity on
411 CO₂ assimilation rates in *Setaria viridis*: a transgenic analysis. *Journal of Experimental
412 Botany*, 68, 299-310.

413 PARRY, M. A. J., ANDRALOJC, P. J., SCALES, J. C., SALVUCCI, M. E., CARMO-SILVA, A. E., ALONSO, H.
414 & WHITNEY, S. M. 2013. Rubisco activity and regulation as targets for crop improvement.
415 *Journal of Experimental Botany*, 64, 717-730.

416 RAINES, C., HARRISON, E. P., OLCER, H. & LLOYD, J. C. 2000. Investigating the role of the thiol-
417 regulated enzyme sedoheptulose-1,7-bisphosphatase in the control of photosynthesis.
418 *Physiologia Plantarum*, 110, 303-308.

419 RAINES, C. A. 2011. Increasing photosynthetic carbon assimilation in C₃ plants to improve crop
420 yield: current and future strategies. *Plant Physiology*, 155, 36-42.

421 RAY, D. K., MUELLER, N. D., WEST, P. C. & FOLEY, J. A. 2013. Yield trends are insufficient to double
422 global crop production by 2050. *PLOS ONE*, 8, e66428.

423 ROSENTHAL, D. M., LOCKE, A. M., KHOZAEI, M., RAINES, C. A., LONG, S. P. & ORT, D. R. 2011. Over-
424 expressing the C₃ photosynthesis cycle enzyme Sedoheptulose-1-7 Bisphosphatase
425 improves photosynthetic carbon gain and yield under fully open air CO₂ fumigation (FACE).
426 *Bmc Plant Biology*, 11, 123-123.

427 SAGE, R. F. & PEARCY, R. W. 1987. The nitrogen use efficiency of C₃ and C₄ plants. II Leaf nitrogen
428 effects on the gas exchange characteristics of *Chenopodium album* L. and *Amaranthus*
429 *retroflexus* L. *Plant Physiology*, 84, 959-963.

430 SALESSE-SMITH, C. E., SHARWOOD, R. E., BUSCH, F. A., KROMDIJK, J., BARDAL, V. & STERN, D. B.
431 2018. Overexpression of Rubisco subunits with RAF1 increases Rubisco content in maize.
432 *Nature Plants*, 4, 802-810.

433 SIMKIN, A. J., LÓPEZ-CALCAGNO, P. E. & RAINES, C. A. 2019. Feeding the world: improving
434 photosynthetic efficiency for sustainable crop production. *Journal of Experimental Botany*,
435 70, 1119-1140.

436 SOUTH, P. F., CAVANAGH, A. P., LIU, H. W. & ORT, D. R. 2019. Synthetic glycolate metabolism
437 pathways stimulate crop growth and productivity in the field. *Science*, 363, eaat9077.

438 VON CAEMMERER, S. 2021. Updating the steady-state model of C₄ photosynthesis. *Journal of*
439 *Experimental Botany*, 72, 6003-6017.

440 VON CAEMMERER, S. & FURBANK, R. T. 1999. Modeling of C₄ photosynthesis. In: SAGE, R. F. &
441 MONSON, R. (eds.) *C₄ plant biology*. San Diego, CA, USA: Academic Press.

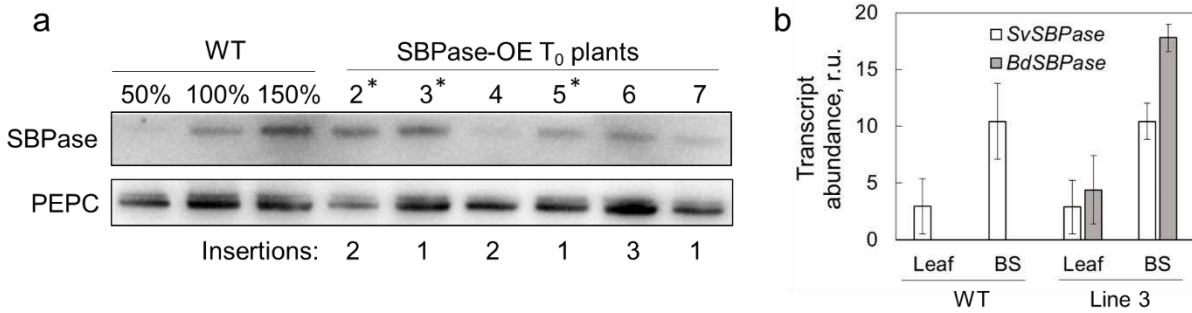
442 VON CAEMMERER, S. & FURBANK, R. T. 2016. Strategies for improving C₄ photosynthesis. *Current*
443 *opinion in plant biology*, 31, 125-134.

444 WALKER, B. J., VANLOOCKE, A., BERNACCHI, C. J. & ORT, D. R. 2016. The Costs of Photorespiration
445 to Food Production Now and in the Future. *Annual Review of Plant Biology*, Vol 67, 67, 107-
446 +.

447 WOODROW, I. E., MURPHY, D. J. & LATZKO, E. 1984. Regulation of stromal sedoheptulose 1,7-
448 bisphosphatase activity by pH and Mg²⁺ concentration. *Journal of Biological Chemistry*,
449 259, 3791-3795.

450

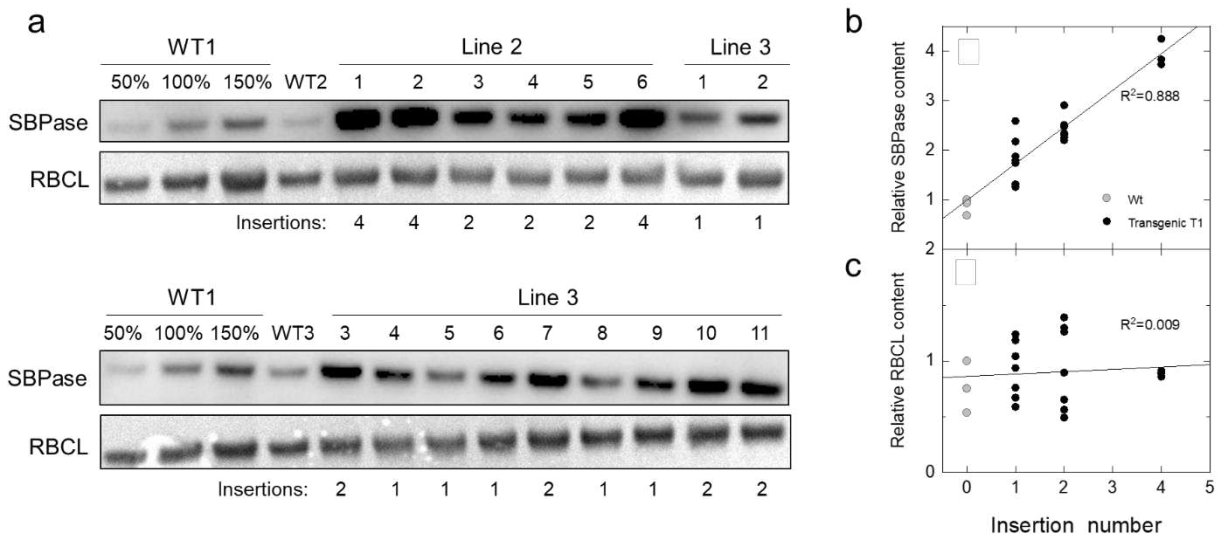
451



452

453 **Figure 1.** Selection of *S. viridis* plants overexpressing SBPase. **a.** Immunoblots of SBPase and PEPC in
454 WT *S. viridis* and 6 T₀ plants transformed with *SBPase* from *Brachypodium distachyon* under the
455 control of the bundle sheath cell-preferential *GLDP* promoter. The *htp* copy numbers estimated by
456 digital PCR and suggesting the *BdSBPase* insertion numbers are also shown. Asterisks indicate the
457 plants which progenies were used in further experiments. **b.** Transcript abundance of *S. viridis*
458 *SBPase* (*SvSBPase*) and *B. distachyon* *SBPase* (*BdSBPase*) in whole leaf tissue and isolated bundle
459 sheath strands (BS) shows bundle sheath-preferential localisation of the native gene and transgene
460 transcripts. Mean \pm SE, $n = 3$ biological replicates.

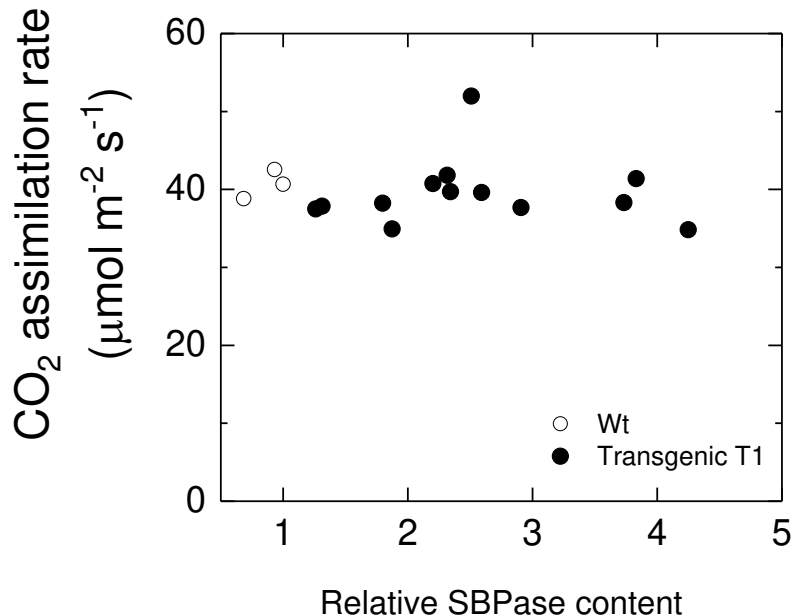
461



462

463 **Figure 2.** Analysis of *S. viridis* plants overexpressing SBPase. **a.** Immunodetection of SBPase and RBCL
464 in protein samples isolated from leaves of WT plants and the T₁ progeny of transgenic lines 2 and 3.
465 Samples were loaded on leaf area basis, and the titration series of the WT1 sample was used for
466 relative quantification. Insertion number indicates *hpt* copy number estimated by digital PCR. **b** and
467 **c.** Relative SBPase and RBCL content as a function of insertion number (data taken from a).

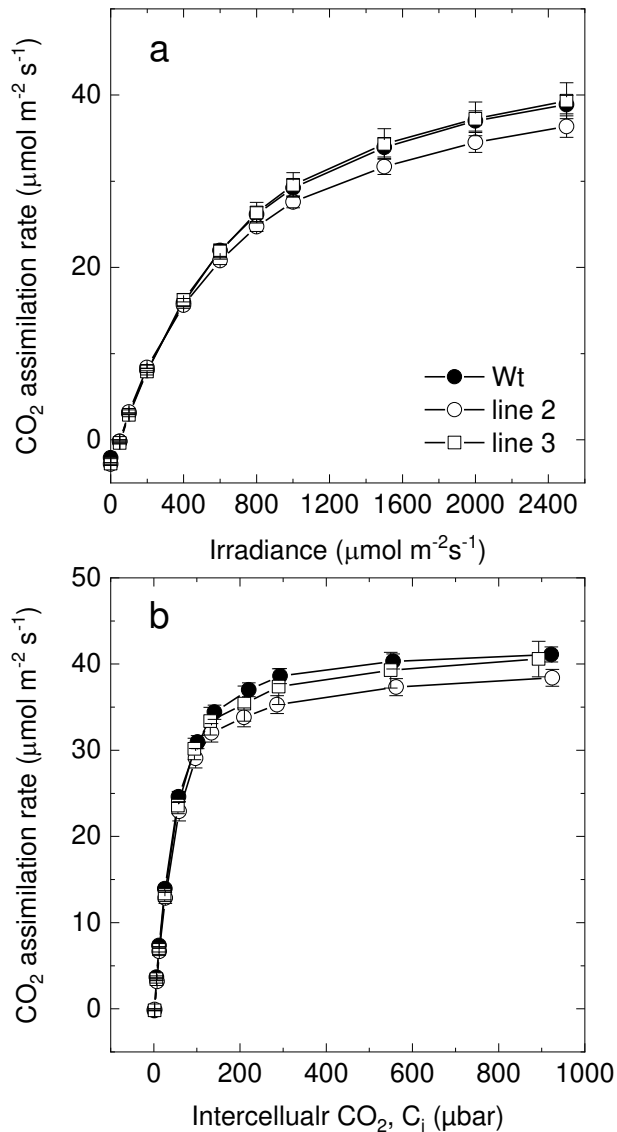
468



469

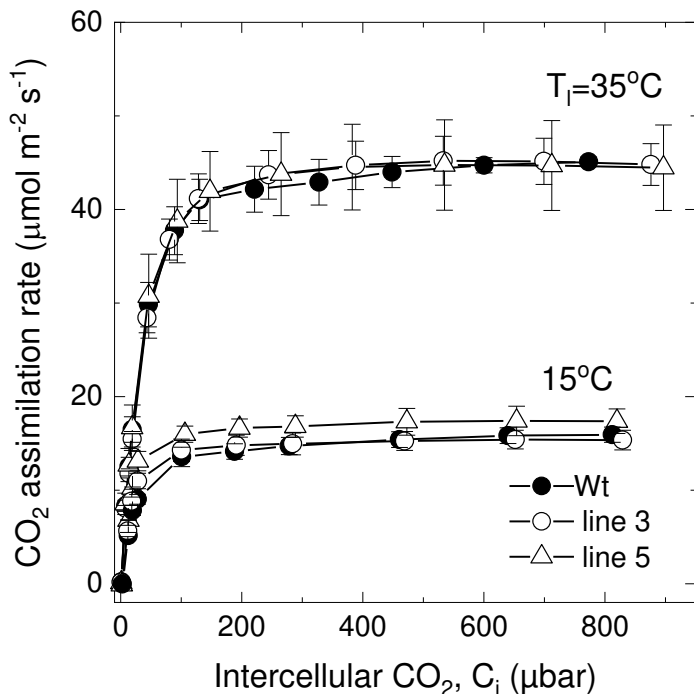
470 **Figure 3.** Saturating CO_2 assimilation rate as a function of relative SBPase content in leaves of WT *S.*
471 *viridis* and T₁ progeny of lines 2 and 3 overexpressing SBPase. Measurements were made at an
472 ambient CO_2 partial pressure of 400 μbar , an irradiance of $1500 \mu\text{mol m}^{-2} \text{s}^{-1}$ and a leaf temperature
473 of 28 °C.

474



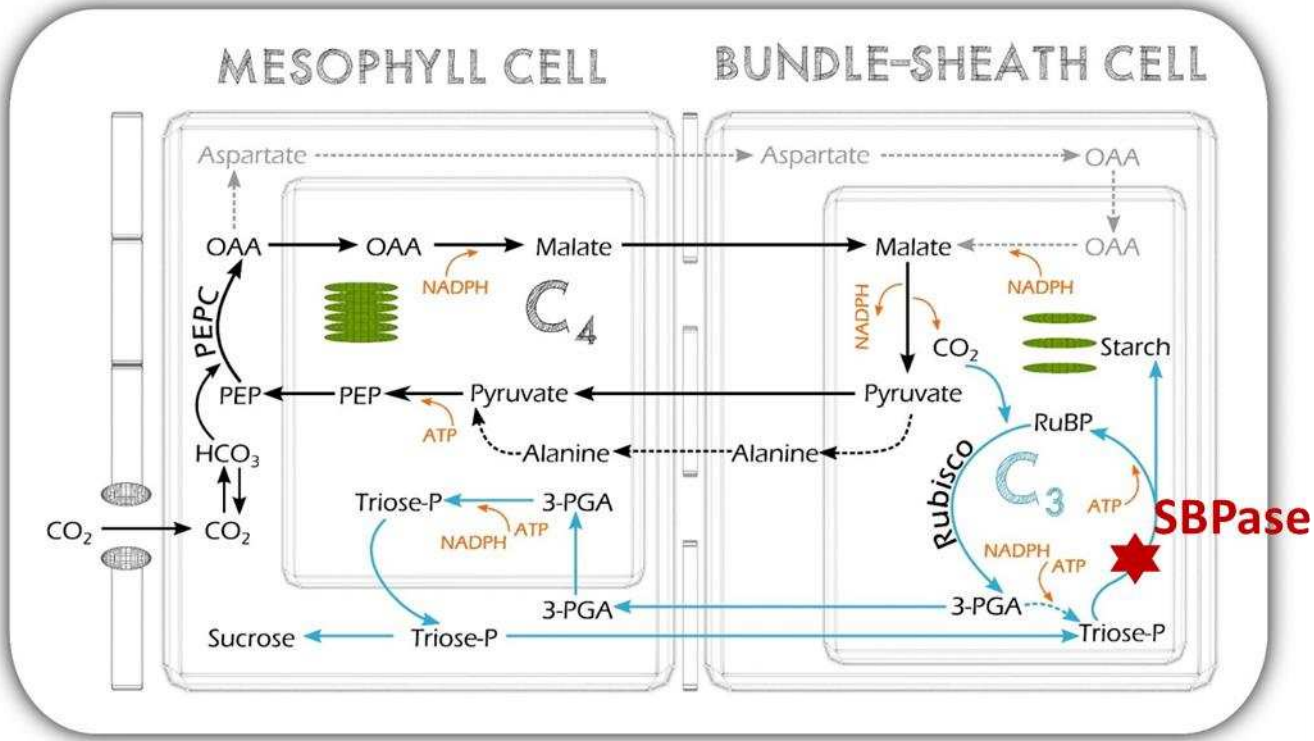
475

476 **Figure 4.** Gas exchange properties of WT *S. viridis* and transgenic plants overexpressing SBPase. **a.** 477 CO₂ assimilation rate as a function of intercellular CO₂ partial pressure. Measurements were made 478 at an irradiance of 1500 μmol m⁻² s⁻¹ and a leaf temperature of 28 °C. **b.** CO₂ assimilation rate as a 479 function of irradiance. Measurements were made at an ambient CO₂ partial pressure of 400 μbar 480 and a leaf temperature of 28 °C. Measurements were made on the T₁ progeny of lines 2 and 3. 481 Average relative abundance of SBPase per leaf area, calculated from immunoblots on Fig. 2, was 482 significantly increased in line 2 (3.2 times, *P* = 0.002) and in line 3 (2.0 times, *P* = 0.001), relative to 483 WT. Mean ± SE, *n* = 3 biological replicates. No significant differences were found (*P* < 0.05). 484



485

486 **Figure 5.** CO₂ assimilation rate as a function of intercellular CO₂ partial pressure at different
487 temperatures in WT *S. viridis* and transgenic plants overexpressing SBPase. Measurements were
488 made at an irradiance of 1500 μmol m⁻² s⁻¹ and a leaf temperature of 35 °C or 15 °C. Measurements
489 were made on the T₂ progeny of lines 3 and 5 and wild type. Average relative abundance of SBPase
490 per leaf area, calculated from immunoblots on Fig. S1, was increased 2 times in line 3 and 1.5 times
491 in line 5, relative to WT. Mean ± SE, n = 3 biological replicates. Details of statistical analysis are
492 provided in the results.



493

494 **Figure 6.** Schematic of the NADP-ME C₄ photosynthetic pathway of *S. viridis* showing the location of
495 SBPase in the pathway.

496